*AAPS PharmSciTech (2019) 20: 64*
DOI: 10.1208/s12249-018-1208-8

*Research Article*

# Formation Mechanism, *In vitro* and *In vivo* Evaluation of Dimpled Exenatide Loaded PLGA Microparticles Prepared by Ultra-Fine Particle Processing System

**Chune Zhu,[1] Tingting Peng,[2] Di Huang,[2,3] Disang Feng,[2] Xinyi Wang,[4] Xin Pan,[2] Wen Tan,[1,5] and Chuanbin Wu[1,2,5]**

*Received 16 August 2018; accepted 1 October 2018; published online 9 January 2019*

***Abstract.*** Spherical poly (D, L-lactic-co-glycolic acid) microparticles (PLGA-MPs) have long been investigated in order to achieve sustained delivery of proteins/peptides. However, the formation mechanism and release characteristics of the specific shape MPs were still unknown. This study aimed to develop a novel-dimpled exenatide-loaded PLGA-MPs (Exe-PLGA-MPs) using an ultra-fine particle processing system (UPPS) and investigate the formation mechanism and release characteristics. Exe-PLGA-MPs were prepared by UPPS and optimized based on their initial burst within the first 24 h and drug release profiles. Physicochemical properties of Exe-PLGA-MPs, including morphology, particle size, and structural integrity of Exe extracted from Exe-PLGA-MPs, were evaluated. Furthermore, pharmacokinetic studies of the optimal formulation were conducted in Sprague-Dawley (SD) rats to establish *in vitro-in vivo* correlations (*IVIVC*) of drug release. Exe-PLGA-MPs with dimpled shapes and uniform particle sizes achieved a high encapsulation efficiency (EE%, 91.50 ± 2.65%) and sustained drug release for 2 months *in vitro* with reduced initial burst (20.42 ± 1.64%). Moreover, the pharmacokinetic studies revealed that effective drug concentration could be maintained for 3 weeks following a single injection of dimpled Exe-PLGA-MPs with high *IVIVC*. Dimpled PLGA-MPs prepared using the UPPS technique could thus have great potential for sustained delivery of macromolecular proteins/peptides.

**KEY WORDS:** exenatide; dimpled; drug release; pharmacokinetics; ultra-fine particle processing system (UPPS).

## INTRODUCTION

The development of biodegradable polymers for long-acting drug delivery systems *via* the parenteral route started in early 1970s (1). More recently, preparation of biodegradable polymer microparticles (MPs), such as poly (D, L-lactic-co-glycolic acid) (PLGA) MPs, have been widely studied for long-acting delivery of proteins/peptides due to their biodegradability, non-toxicity, and ability to slowly release encapsulated drugs in a controlled manner over a prolonged period of time following a single administration (2,3). PLGA-MPs thus have the potential to maintain efficient drug concentrations at the target site and minimize side effects induced by frequent injections (4,5). So far, a number of commercial products based on PLGA-MPs have been approved by the Food and Drug Administration (FDA), including Lupron Depot® (leuprolide), Trelstar® (triptorelin), Risperidal Consta® (risperidone), and Zoladex® implant (goserelin acetate) (6,7).

The commonly used methods for fabrication of drug loaded PLGA-MPs include conventional water in oil in water (W/O/W) emulsion solvent evaporation technique and its alternatives, such as solid in oil in water (S/O/W) and water in

**Electronic supplementary material** The online version of this article (https://doi.org/10.1208/s12249-018-1208-8) contains supplementary material, which is available to authorized users.

[1] Guangdong University of Technology, Institute for Biomedical and Pharmaceutical Sciences, Guangzhou, 510006, China.
[2] School of Pharmaceutical Sciences, Sun Yat-sen University, Guangzhou, 510006, China.
[3] *Present Address:* Buchanan Ocular Therapeutics Unit, Department of Ophthalmology, New Zealand National Eye Centre, Faculty of Medical and Health Sciences, The University of Auckland, Private Bag 92019, Auckland, 1142, New Zealand.
[4] Guanghua School of Stomatology, Hospital of Stomatology, Sun Yat-sen University, Guangzhou, 510055, China.
[5] To whom correspondence should be addressed. (e–mail: went@gdut.edu.cn; wuchuanb@mail.sysu.edu.cn; )

oil in oil (W/O/O) methods (8). In addition, novel techniques, such as ultrasonic atomization, spray drying, and membrane emulsification, have also been developed to prepare PLGA-MPs (9,10). However, all the methods have disadvantages, including low encapsulation efficiency (EE%), high initial burst release, unclear drug release mechanisms, impaired bioactivity of therapeutic proteins/peptides in the PLGA matrix during preparation (11).

The ultra-fine particle processing system (UPPS) was a novel technique of MP preparation based on the disk rotation principle, originally designed by our research group (12). It is mainly consisted of four parts, including a center feed inlet nozzle with a diameter of 0.7 mm, a rotating disk, an airflow system, and 12 sample collection plates (13). Figure 1 shows the working process of preparation of proteins/peptides loaded PLGA-MPs using UPPS.

Compared to conventional preparation methods, UPPS is able to prepare MPs with different shapes and sizes, achieve a high EE%, reduce the initial burst release, protect the bioactivity of proteins/peptides, and control drugs released from MPs. Previously, a variety of particulate formulations, including enhanced green fluorescent protein-loaded silk fibroin microspheres and risperidone-loaded PLGA microspheres have been successfully prepared using UPPS (12,14). More recently, a preliminary study on the comparison of exenatide loaded PLGA-MPs (Exe-PLGA-MPs) prepared by UPPS and spray drying techniques was reported (13). However, effects of morphology of PLGA-MPs on *in vitro* drug release and *in vivo* pharmacokinetics remain unclear.

Exe, a peptide composed of 39 amino acids, was used as a model drug in this study. It is a glucagon-like peptide-1 (GLP-1) receptor agonist and used for the treatment of type 2 diabetes (15). According to the World Health Organization (WHO) report, there will be more than 300 million diabetic people worldwide in 2025 with over 95% of patients suffering from type 2 diabetes (16,17). A great effort has to be made to develop long-acting Exe delivery systems in the treatment of type 2 diabetes.

In this study, Exe-PLGA-MPs with dimpled shapes were prepared by UPPS to achieve improved EE%, reduced initial burst release, and controlled drug release. Additionally, the mechanism of formation of dimpled Exe-PLGA-MPs was investigated and pharmacokinetic studies were also performed to evaluate the *in vitro-in vivo* correlations (*IVIVC*) of the optimal formulation.

## MATERIALS AND METHODS

### Materials

Exenatide with purity > 98.0% by HPLC analysis was purchased from Jill Biochemical co., Ltd., (China). Free-acid terminated PLGA with a 50/50 ratio of lactic to glycolic acid (Mw = 40,000) was gained from Daigang Biology (China). Biomarkers were purchased from Thermo Fisher Scientific (USA). The Exendin-4 kits were purchased from Phoenix Pharmaceuticals, Inc. (USA). All other reagents used in this study were analytical grade and the deionized water was used throughout the research.

### Preparation of Exe-PLGA-MPs by UPPS

Exe-PLGA-MPs were prepared by UPPS. As described in Fig. 1, PLGA was dissolved in an organic phase composed of dichloromethane (DCM) and dimethyl carbonate (DMC) with a volume ratio of 1:1 or only DCM to obtain the oil phase with a polymer concentration of 3.0% (*w*/*v*). Exe (6, 12, 12, and 18 mg) was dissolved in 1.0 mL deionized water to obtain the aqueous phase and a number of formulations (F1, F2, F3, and F4) with theoretical drug loading (DL%) of 1.0%, 2.0%, 2.0%, and 3.0%, respectively, were prepared. For F3, the organic phase was DCM only. The aqueous phase was then mixed with the oil phase at a volume ratio of 1:20 and immediately emulsified using a probe ultrasonic processor (JY92-2D, Ningbo, China) at a power of 400 watt on an ice bath for 30 s to form primary water in oil (W/O) emulsions. Subsequently, the primary emulsions were pumped to the center feed inlet nozzle of UPPS through a peristaltic pump (EYELA MP-100, Japan) at a feeding rate of 3 mL/min and MPs were formed on the rotating disk at 15000 rpm. The resulting MPs were collected from sample collection plates and lyophilized with the cold trap temperature − 50 °C and vacuum 0.25 mbar for 12 h (Christ, Alpha 1-4 LSC, Germany).

### Characterization of Exe-PLGA-MPs

#### *Determination of EE%*

Three batches of MPs (F1 to F4) were prepared and their DL% was measured. Briefly, 10 mg of MPs were

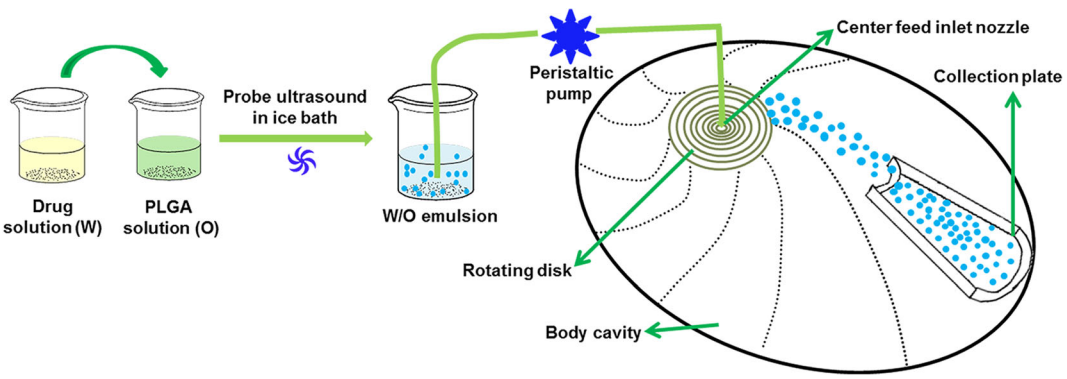


**Fig. 1.** The flow chart of PLGA loaded protein/peptide microparticles prepared by UPPS

weighed precisely, dissolved in 1 mL of DCM, vortexed for 30 s, and centrifuged at 12,000 rpm for 5 min. The precipitate was dried in a thermostatic vacuum drier for 2 h to evaporate residual solvents and dissolved in PBS (pH 7.4). The concentration of Exe was measured by HPLC at 30 °C on a Phenomenex Gemini C18 chromatographic column (110A, 250 × 4.6 mm, 5 μm) with a gradient elution method. The mobile phase A was acetonitrile containing 0.1% (*v*/*v*) trifluoroacetic acid at the flow rate of 1.0 mL/min and the mobile phase B was ultrapure water with 0.1% (*v*/*v*) trifluoroacetic acid. The UV absorbance was at the wavelength of 220 nm and each sample was injected with a volume of 20 μL. A calibration curve of Exe concentrations was made within the range of 15~1000 μg/mL ($R^2 = 0.9997$). Each sample was measured in triplicate and data was expressed as the mean ± standard deviation (S. D.). The EE% was defined as Eq. 1 (18):

$$EE\% = \frac{M_{\text{actual drug loading}}}{M_{\text{theoretical drug loading}}} \times 100\% \quad (1)$$

*Morphology and Particle Size*

Morphology of Exe-PLGA-MPs was visualized using scanning electron microscopy (SEM, JSM-6330F, JEOL Ltd., Japan). The samples were fixed on a SEM-stub using double-sided adhesive tapes and then sputter coated with a thin layer of gold under vacuum before observation.

The particle size of F1 to F4 was analyzed using a Master-sizer 2000 laser particle analyzer (Malvern Instruments Ltd., Malvern, UK). The size distribution was defined using $S_{pan}$ values and was calculated according to Eq. (2), where $D_{0.9}$, $D_{0.1}$, and $D_{0.5}$ were volume size diameters at 90%, 10%, and 50% of the cumulative volume, respectively.

$$S_{pan} = \frac{D_{0.9} - D_{0.1}}{D_{0.5}} \quad (2)$$

*In vitro Drug Release*

An amount of 10 mg of Exe-PLGA-MPs were dispersed in 1 mL of phosphate buffer saline (PBS, pH 7.4) under stirring at 37 °C and shaking at 100 rpm. At predetermined time points, supernatants were collected after centrifugation for 5 min at 5000 rpm and replaced with an equal volume of fresh medium. The concentration of Exe in the supernatant was analyzed by HPLC as described above. The optimal formation was further investigated in the subsequent studies.

*Sodium Dodecyl Sulfate-Polyacrylamide Gel Electrophoresis (SDS-PAGE) Analysis*

The structural integrity of Exe extracted from F2 was detected by SDS-PAGE. The concentrations of acrylamide separating gel (pH 8.8) and stacking gel (pH 6.8) were 16% and 4% (*w*/*v*), respectively. All the samples were heated up in boiling water for 5 min and electrophoresed at voltage of 100 V. After migration, the gel was stained with Coomassie Bright Blue R250 for 1 h, de-stained, and detected using the automatic gel image system (Tanon 4500sf Tanon Science & Technology Co., Ltd., China).

*Laser Micro-Raman Spectroscopy*

Raman spectroscopy is used to identify the difference between the incident and scattered radiation frequencies based on the types of bonds and modes of vibration (19). In this study, Exe, Exe-PLGA-MPs (F2), and PLGA matrix were sown on glass slides and analyzed using a Raman microscope (Renishaw Invia Raman Microscope, UK). The spectrograms were acquired in the range of 500–4000 $cm^{-1}$ by accumulating 32 scans at a resolution of 4 $cm^{-1}$ (20).

*Synchrotron Radiation X-Ray-Computed Microtomography (SR-μCT)*

The three-dimensional (3D) internal structure of Exe-PLGA-MPs (F2) was analyzed by SR-μCT with a beam line of BL13W1 as previously described by Guo *et al* (21). Samples were scanned at 13.0 KeV and the distance between sample and detector was set at 12.0 cm. Projections were magnified by diffraction-limited microscope optics (× 10 magnification) and digitized with an efficient pixel size of 0.65 μm (ORCA Flash 4.0 Scientific CMOS, Hamamatsu K.K., Shizuoka Pref., Japan). The exposure time was 1.0 s and the number of flat gap was 120. The 3D data of MPs was analyzed by the VGStudio Max (Version 2.1, Volume Graphics GmbH, Germany) and Image Pro Analyzer 3D (version 7.0, Media Cybernetics, Inc., USA) software.

## *In vivo* Studies

*Pharmacokinetics*

Pharmacokinetics of Exe-PLGA-MPs (F2) were investigated in Sprague-Dawley (SD) rats. Animals were sourced from the Laboratory Animal Center of Sun Yat-sen University and all experimental procedures were in accordance with National Institute of Health and Nutrition Guidelines for the Care and Use of Laboratory Animals. Rats were raised in rooms at 25 ± 1 °C and 55 ± 5% relative humidity under a normal cyclic light condition (12 h light/dark) and received *ad libitum* chow diet and water during acclimatization.

A total of 18 male SD rats weighing between 250 and approximately 300 g were divided into three groups ($n = 6$): the positive and negative control groups were received a single subcutaneous injection of Exe solution (drug dosage 100 μg/kg) and saline, respectively. The residual rats were received a single subcutaneous injection of Exe-PLGA-MPs suspension (the medium containing 0.87% of NaCl, 0.75% of CMC-Na, and 0.1% of Tween 20) with the amount of total drugs equivalent to twice-daily injections of Exe solution for 15 days (22). After injection, blood samples were collected using ice-cold tubes containing anticoagulant (heparin solution, 5000 U/mL) at predetermined time points. All the blood samples were rapidly centrifuged at 3500 rpm for 15 min and 100 μL of plasma was analyzed using an Exendin-4 EIA kit (EK-070-94, Phoenix pharmaceuticals, USA) (23).

**Table I.** Characteristics of Exe-PLGA-MPs Prepared by UPPS (F1 to F4, $n = 3$)

| Formulation | Oil phase | Theoretical DL (%) | Actual DL (%) | EE% | Median particle diameter (μm) | PDI | $S_{pan}$ value |
|---|---|---|---|---|---|---|---|
| F1 | DCM + DMC | 1.0 | 0.92 ± 0.02 | 92.00 ± 3.08 | 36.33 ± 3.31 | 0.19 ± 0.04 | 1.76 ± 0.19 |
| F2 | DCM + DMC | 2.0 | 1.83 ± 0.07 | 91.50 ± 2.65 | 33.99 ± 2.11 | 0.15 ± 0.03 | 1.48 ± 0.13 |
| F3 | DCM | 2.0 | 1.79 ± 0.10 | 89.50 ± 2.87 | 27.64 ± 3.05 | 0.27 ± 0.05 | 2.26 ± 0.24 |
| F4 | DCM + DMC | 3.0 | 2.69 ± 0.11 | 89.67 ± 3.56 | 35.91 ± 3.59 | 0.24 ± 0.06 | 1.91 ± 0.22 |

DL% represents drug loading, EE% represents encapsulation efficiency, and PDI represents polydispersity index

Pharmacokinetic parameters, including the maximum Exe concentration plasma ($C_{max}$), time to maximal plasma concentration ($T_{max}$), terminal half-life ($T_{1/2}$), and the area under the concentration-time curve (AUC) were determined using WinNonlin Professional software (Version 5.1) (24). The apparent elimination rate constant ($K_{el}$) was also calculated through the least-squares regression analysis.

*Relative Bioavailability (RB%)*

The mean RB% of formulations was analyzed through the AUC based on the trapezoidal rule. In this study, the RB% of MPs was calculated by comparing the subcutaneous injection of Exe-PLGA-MP suspension to Exe solution in rats according to the following equation (25):

$$\mathrm{RB}\ (\%) = \frac{[\mathrm{AUC}]_A/\mathrm{dose}_A}{[\mathrm{AUC}]_B/\mathrm{dose}_B} \times 100\% \tag{3}$$

where *A* and *B* represent Exe-PLGA-MP suspension and Exe solution, respectively.

*IVIVC*

The data generated from *in vitro* drug release and *in vivo* pharmacokinetic studies were used to future investigate the *IVIVC* of Exe-PLGA-MPs (2,26). The fraction of drug absorbed *in vivo* was determined using Eq. (4) and its correlation with *in vitro* drug release properties was examined.

$$\textit{Invivo}\ \text{cumulative release}(\%) = \frac{\mathrm{AUC}_{0\sim t}}{\mathrm{AUC}_{0\sim 30d} + \dfrac{A\mathrm{UC}_{30d}}{K_{el}}} \times 100 \tag{4}$$

The AUC was calculated based on the linear trapezoidal rule and $K_{el}$ was evaluated through the least-squares regression analysis with the values of correlation coefficient ($R^2$), slope, and intercept.

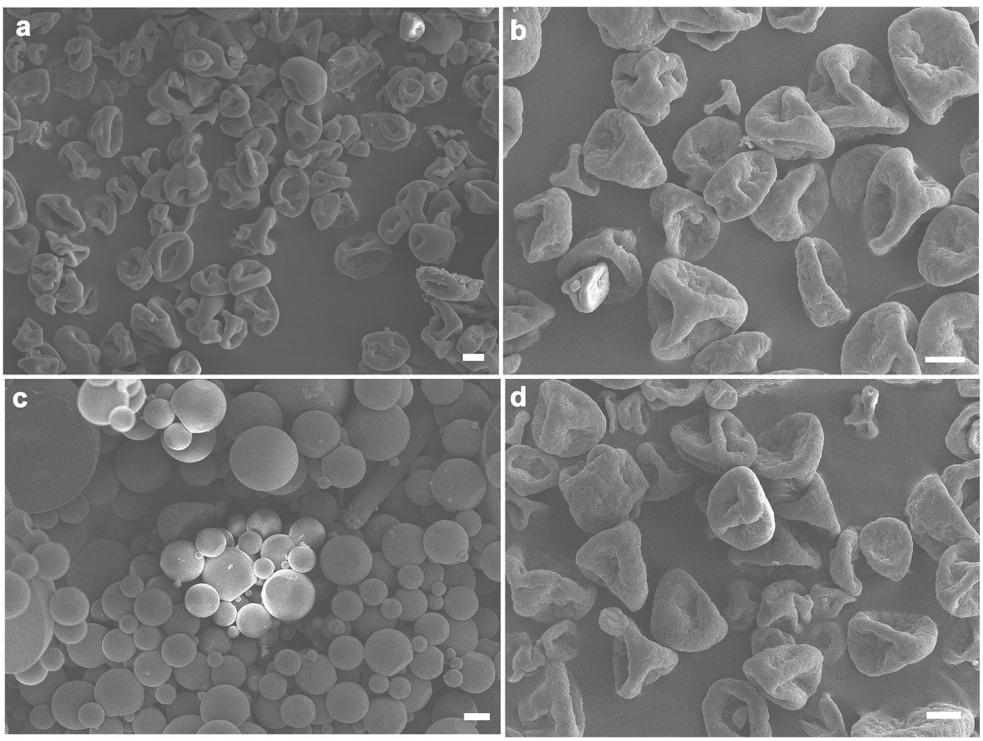


**Fig. 2.** SEM images of Exe-PLGA-MPs, from (**a**) to (**d**) was the images of F1 to F4, the scale bar was 10 μm

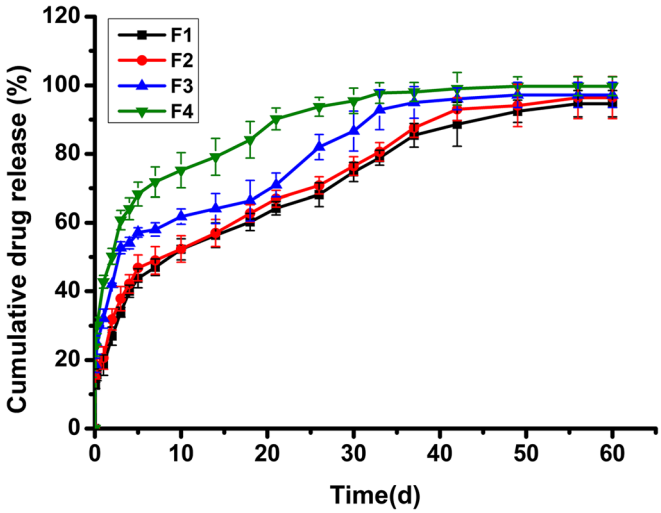


**Fig. 3.** Cumulative *in vitro* drug release profiles of Exe-PLGA-MPs prepared by UPPS in PBS (pH 7.4) (mean ± S.D., $n = 3$)

### Statistical Analysis

Statistical analysis was performed using one-way ANOVA followed by a Dunnett test using IBM SPSS statistics software (version 19.0). All experimental results were obtained in triplicates and the data represent as the mean ± S. D. Statistical difference between the experimental and control groups was considered significant if $p < 0.05$.

## RESULTS

### Characteristics of Exe-PLGA-MPs

*EE%, Particle Size Distribution and Morphology of Exe-PLGA-MPs*

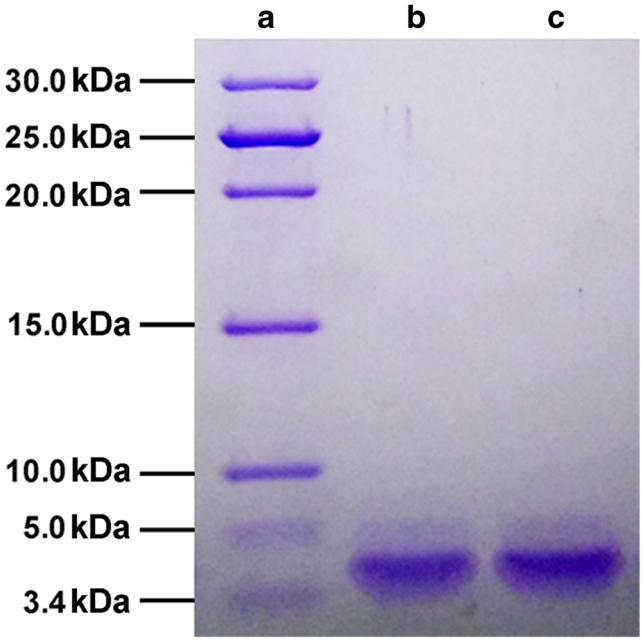


**Fig. 4.** SDS-PAGE analysis of biomarker (**a**), original Exe solution (**b**), and Exe extracted from Exe-PLGA-MPs (F2, **c**)

Table I displays physicochemical characteristics of Exe-PLGA-MPs, including DL%, EE%, and particle size distribution. The particle size of MPs was not affected by the different theoretical DL%, showing a median particle diameter in the range of 27~37 μm. Moreover, F1, F2, and F4 showed a narrow size distribution with the $S_{pan}$ values less than 2.0, indicating that UPPS could prepare MPs with uniform particle sizes. However, F3, which was prepared without the addition of DMC in the oil phase, exhibited a smaller particle size and a larger $S_{pan}$ value compared to other three formulations. Figure 2 shows SEM images of MPs, with F1, F2, and F4 exhibiting a dimpled morphology with sags and pores on the particle surface and F3 displaying as spheres with smooth surfaces.

*In vitro Drug Release*

Figure 3 shows *in vitro* drug release profiles of Exe-PLGA-MPs. All four formulations achieved sustained drug release over 2 months with a cumulative amount of released drugs of 95%. However, the obvious initial burst release was observed within 24 h with increasing theoretical DL%. More than 40% of encapsulated drugs were quickly released from F4 (theoretical DL% of 3.0%). F1 and F2, on the other hand, showed reduced initial burst of approximately 18% and 20%, respectively. It also was noticed that F3 (theoretical DL% of 2.0%) showed a more significant initial burst compared to the F2, with 32% of encapsulated drugs released within the first 24 h.

*SDS-PAGE Analysis*

Biomarkers with MW between 3.4 and 30 kDa were used in this experiment and their bands on SDS-PAGE were shown in Fig. 4A. Both Exe solution (Fig. 4B) and Exe extracted from MPs (Fig. 4C) migrated as a single band within the range of MW between 3.4 and 5.0 kDa. It is believed that the MW of Exe was not changed during the preparation process (27,28).

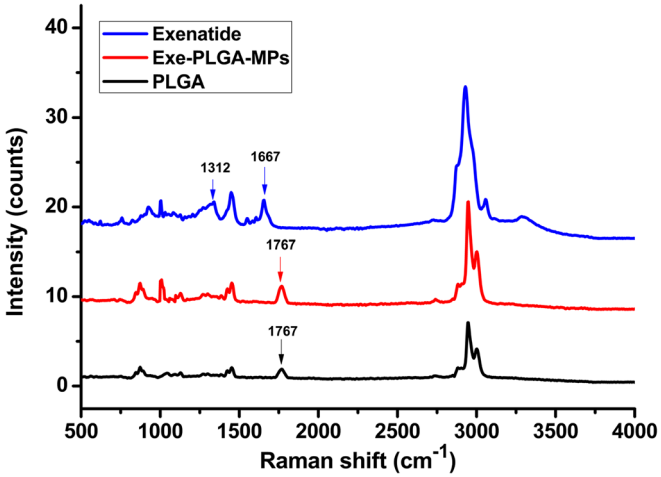


**Fig. 5.** Raman spectra of Exe, Exe-PLGA-MPs (F2) and PLGA

*Laser Micro-Raman Spectroscopy Analysis*

Characteristic Raman bands of proteins generally include amide I (C=O stretch, about 1650 $cm^{-1}$), II (N–H bend and C–N stretch, about 1550 $cm^{-1}$) and III bands (C–N stretch and N–H bend, about 1300 $cm^{-1}$) with the amide I and III bands indicating α-helical and/or β-sheet structures of proteins, respectively (19). The specific wavenumbers of vibrational bands are dependent on inter- and intramolecular effects of characteristic groups, including hydrogen-bonding patterns and peptide-bond angles. Thus, vibrational spectra can be used to analyze the secondary structure of peptides/proteins by inspection of frequency of amide bonds.

Representative Raman spectra of Exe, Exe-PLGA-MPs (F2), and PLGA are shown in Fig. 5. Exe exhibited two characteristic bands of amide I and III at 1667 $cm^{-1}$ and 1312 $cm^{-1}$, respectively, which were attributed to the α-helical and/or β-sheet conformation (12,20). The band of Raman spectra for PLGA was at 1767 $cm^{-1}$. No characteristic bands of Exe were shown in the spectrum of F2, whereas all the representative band of PLGA showed up. These results confirmed that Exe was completely encapsulated into MPs without any interaction with PLGA matrix.

*SR-μCT Analysis*

Morphology of F2 prepared by UPPS was further characterized using SR-μCT. Figure 6a shows the overall structure of MPs preliminarily in two-dimensional (2D) images. Compared with 2D images with a relatively low resolution, 3D images (Fig. 6b, c) allowed a direct observation. MPs prepared by UPPS possessed a dimpled morphology and a particle size of 34 μm, which were consistent with the results obtained by SEM and laser particle analyzer. Figure 6d indicates a 3D image of individual MPs, showing a dimpled morphology with a small amount of internal cavities. Compared to SEM, SR-μCT has huge advantages in 2D and 3D visualization of internal and external geometrical structures of MPs due to its high resolution and contrast (29).

## *In vivo* Studies

*Pharmacokinetic Study*

Figure 7a shows the Exe concentration in plasma to time profiles of Exe-PLGA-MPs (F2) and Exe solution. The saline was injected as a negative control with the drug concentration in plasma showing zero at all the time points (data not shown). After injection of Exe solution, the drug concentration in plasma showed a dramatic increase to a peak value (the $C_{max}$ was 135.34 ± 13.26 ng/mL) at 2 h and followed by a decrease to 3.79 ± 1.25 ng/mL within 12 h (Table II). In contrast, the drug concentration in plasma was constantly maintained at a high level within about 3 weeks post administration of Exe-PLGA-MPs, though the $C_{max}$ (103.93 ± 13.79 ng/mL) was a slightly lower than that of Exe injection, demonstrating that slowly released Exe was able to provide therapeutic efficacy for a prolonged period of time. The $AUC_{0-\infty}$ and mean residence time (MRT) of Exe-PLGA-MPs were 316.85 ± 12.59 ng d $mL^{-1}$ and 8.68 ± 0.59 d, respectively, while the corresponding values of Exe solution were 21.92 ± 3.12 ng d $mL^{-1}$ and 0.17 ± 0.05 d, respectively.

*The RB%*

The RB% of Exe-PLGA-MPs in SD rats was calculated according to Eq. (3) and compared to that of Exe solution (25,26). Based on the AUC and dosage values, the estimated RB% of Exe-PLGA-MPs to Exe solution was 96.37 ± 6.45%, suggesting a good reliability in bioequivalence. Additionally, Exe-PLGA-MPs could also have advantages in reduction of injection frequency and thereby increasing patient's compliance compared to administration of Exe solution.

*IVIVC*

The *IVIVC* of Exe-PLGA-MPs was established by profiles of cumulative drug release *in vitro* and *in vivo* with $R^2$ of 0.9853, suggesting a good linear regression correlation (Fig. 7b). Results also indicated that drugs were released from Exe-PLGA-MPs *in vivo* faster than *in vitro* due to the complex microenvironment *in vivo* (1), which was confirmed

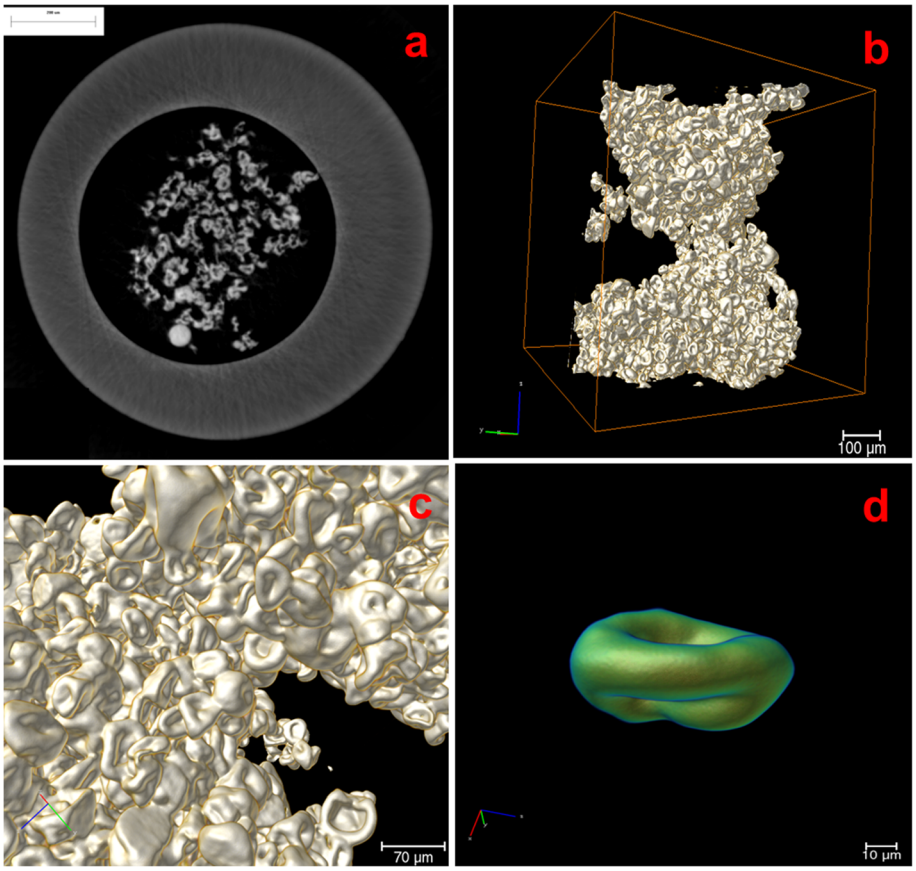


**Fig. 6.** Morphology of Exe-PLGA-MPs (F2) characterized by SR-μCT (**a**: 2D images; **b** and **c**: 3D images; **d**: 3D image of a single microparticle)

by the relationship of released drugs *in vitro* and absorbed drugs *in vivo* ($Y = 0.74X + 3.79$). Therefore, it seemed feasible to predict the *in vivo* drug release rate through the established correlation according to the *in vitro* data (2,26).

## DISCUSSION

In the present work, Exe was encapsulated into PLGA-MPs through the UPPS technique and effects of special morphology of Exe-PLGA-MPs on their EE% and drug release were studied. As shown in Table I, EE% of all formulations was higher than 85%, as the aqueous phase could be uniformly distributed into the oil phase without causing any drug leakage during the preparation process. It was observed that changes in the component of oil phase (removal of DMC) and the resulting morphology did not induce significant differences ($p \geq 0.05$) in the encapsulation efficiency as well as total drug loading of formulations (F2

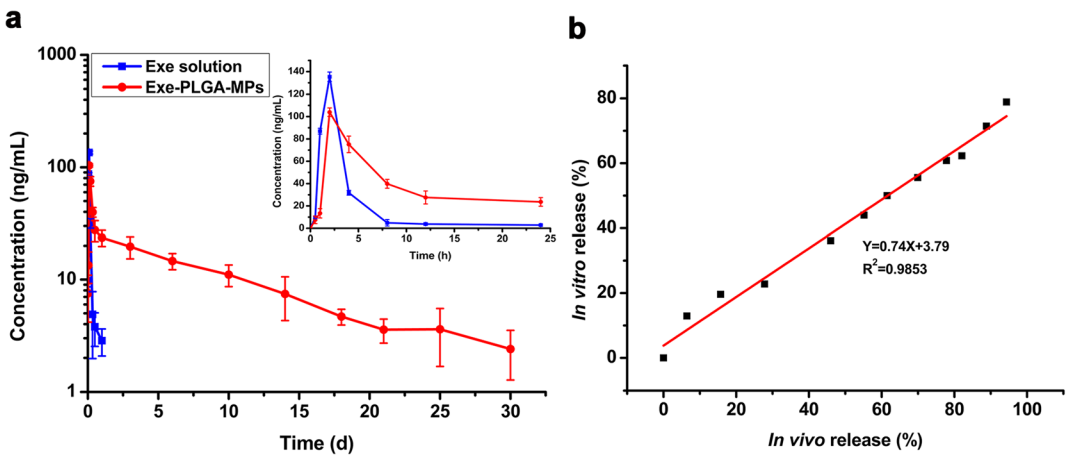


**Fig. 7.** **a** Mean plasma Exe concentration-time curve after subcutaneous injection of Exe-PLGA-MPs (F2) and Exe solution in SD rats, the insert presents the plasma Exe concentration-time within 24 h ($n = 6$); **b** *IVIVC* for Exe-PLGA-MPs (F2)

**Table II.** Pharmacokinetics Parameters of Exe Solution and Dimpled Exe-PLGA-MPs After Subcutaneous Injection in SD rats ($n = 6$)

| Pharmacokinetic parameters | Values | |
|---|---|---|
| | Exe solution | Exe-PLGA-MPs |
| Tmax (h) | 2.00 | 2.00 |
| Cmax (ng $mL^{-1}$) | 135.34 ± 13.26 | 103.93 ± 13.79 |
| $AUC_{0\sim1}$ (ng d $mL^{-1}$) | 18.14 ± 2.77 | 33.23 ± 1.41 |
| $AUC_{0\sim30}$ (ng d $mL^{-1}$) | / | 287.30 ± 11.64 |
| $AUC_{0\sim\infty}$ (ng d $mL^{-1}$) | 21.92 ± 3.12 | 316.85 ± 12.59 |
| $T_{1/2}$ (h) | 3.22 ± 0.23 | 165.33 ± 3.56 |
| MRT (h) | 4.08 ± 0.45 | 208.32 ± 7.59 |
| Ke ($h^{-1}$) | 0.22 ± 0.04 | 0.0042 ± 0.02 |

and F3). However, a significant difference ($p < 0.05$) in drug loading capacity was observed when the theoretical drug loading was also changed from 2% (F3) to 3% (F4). It was probably due to the smaller particle size rather than the dimpled morphology. The mechanism of formation of dimpled MPs (F1, F2, and F4) was competitive interactions between solvent evaporation and solute precipitation (30), which could be due to the difference of boiling point and surface tension of DCM and DMC. The primary emulsions were initially dispersed from the center of disk to the edge and a thin film was formed under the centrifugal force. Subsequently, the thin liquid film was split into micro-droplets (Fig. 8a) and localized in the UPPS body cavity. The outermost layer of solvent was rapidly evaporated under airflow and the solute was eventually precipitated to form a solid membrane onto the surface of micro-droplets (Fig. 8b). However, DCM could be evaporated more quickly due to its low boiling point (39.8 °C) and high surface tension (23.11 dyn/cm), while the corresponding values of DMC is 90.1 °C and 1.29 dyn/cm, respectively. The difference in evaporation rates between two solvents thus resulted in the rough surface of solid membrane. Afterwards, the internal solvent underwent rapid evaporation (Fig. 8c) and the spherical particles gradually collapsed with formation of sags and pores on the surface (Fig. 8d). F3, on the other hand, exhibited spherical shapes and smooth surfaces due to the consistent rate of solvent evaporation.

The initial burst release from MPs increased with increasing theoretical DL% from 1.0 to 3.0%. When the amount of encapsulated drugs was over the maximum DL% capacity of MP carriers, redundant drugs would be attached or absorbed onto the surface of MPs, which might result in a high initial burst. Within the PLGA microparticulate system used in this study, the maximum DL% of Exe was approximately 2.0%. However, F3 with spherical shapes showed a more significant initial burst compared to F2 due to their smaller particle size and non-uniform particle size distribution with the $S_{pan}$ value of 2.26 ± 0.24. The surface area to volume ratio was inversely proportional to the particle size with the smaller particle size accelerating the rate of drug release (31). Therefore, F2 with a high DL% and a reduced initial burst was chosen as the optimal formulation and was further investigated in the following studies.

The regular spherical PLGA-MPs, for example F3 in this work, typically show a typical tri-phasic drug release profile, including a high initial burst caused by the rapid release of drugs adsorbed on the surface of MPs, a constantly slow release period, and a final rapid release phase due to erosion-accelerated degradation of PLGA matrix (32). Unlike conventional MPs, F2 showed a constantly slow drug release behavior with a reduced initial burst, which might be related to their special morphology (Fig. 8e~g). Compared to spherical MPs, dimpled MPs had a relatively large surface area, which could improve the ability of water absorption and facilitate drug release in a diffusion-controlled manner. The drugs adsorbed on the surface or encapsulated in the outermost layer of MP carriers were quickly dissolved in the release medium by absorption of water at the earliest stage of drug release (Fig. 8e). With enhanced ability of water absorption, the resulting hydrolysis of ester bonds in PLGA matrix led to glycolic/lactic production and an acid microenvironment, which further accelerated the hydrolysis process (Fig. 8f).

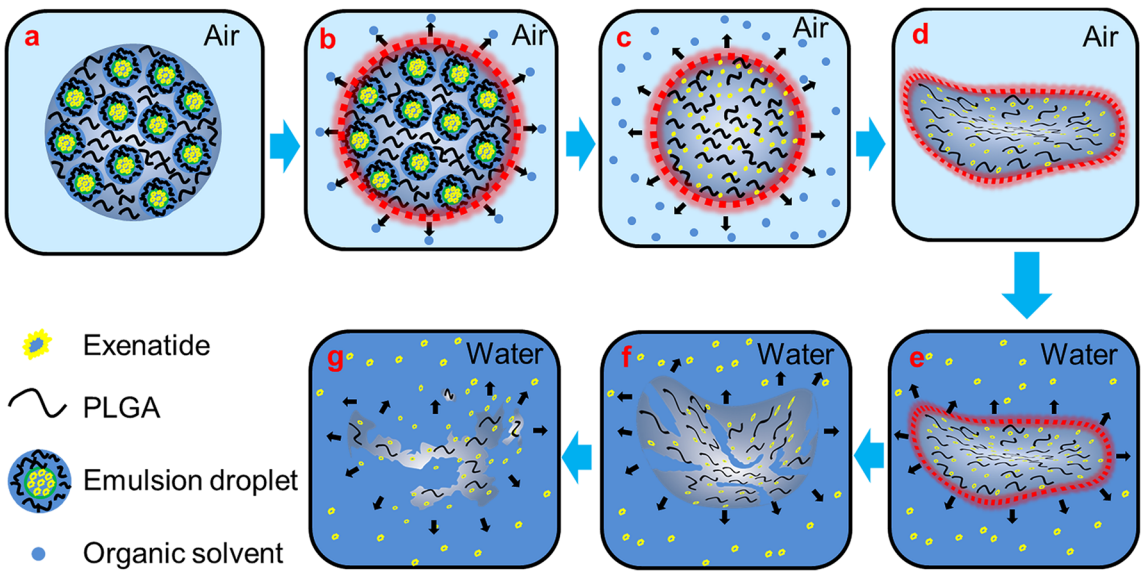


**Fig. 8.** Formation mechanism of dimpled Exe-PLGA-MPs (**a-d**) and drug released from the MPs (**e-g**)

Subsequently, surface/bulk erosion of oligomers and monomers originated from PLGA polymers occurred, which induced further collapse of MPs and constantly sustained drug release (Fig. 8g) (4,33). It is thus believed that both mechanisms of drug diffusion and PLGA erosion regulated drugs release of dimpled MPs, which was confirmed by fitting results. The highest coefficient ($R^2 = 0.9875$) was observed when the drug release profile was fitted with the Korsmeyer-Peppas model, suggesting diffusion and erosion co-induced drug release from MPs. The dimpled morphology of MPs prepared by UPPS has great potentials to provide a paradigm for the design of sustained drug release delivery systems (34).

In the pharmacokinetic study, the drug concentration in plasma was constantly maintained at a high level for 3 weeks after injection of Exe-PLGA-MPs (F2), demonstrating that slowly released Exe provided an efficient therapeutic concentration for a prolonged period of time. It is commonly believed that degradation of PLGA-MPs accelerates drugs release *in vivo* due to the foreign body response against injected MPs and changes in the local environment induced by accumulated endogenous substances, such as enzymes and acidic (1). Similar findings were observed in this work, the rate of drug release was faster *in vivo* (about 21 days) than that in the release medium *in vitro* (more than 35 days). Moreover, the pH value at the injection site might also affect the rate of drug release. According to Doty's report, a lower pH value may catalyze the hydrolysis progress of PLGA and cause accelerated degradation of carriers and drug release (35). The release medium was periodically replaced by fresh PBS in the *in vitro* drug release assay with the pH value consistently maintained at 7.4, whereas erosion and degradation products *in vivo*, including glycolic and lactic, could change the pH value at the injection site and lead to accelerated drug release.

The $C_{max}$ of Exe-PLGA-MPs was lower than that of Exe solution due to the reduced initial burst, which could benefit to the safety of formulations and reduce the potential risks of dose dumping. The enhanced AUC and MRT of Exe-PLGA-MPs also resulted from their sustained drug release behavior. Administration of Exe solution, on the other hand, exhibited a relatively high rate of absorption due to the rapid elimination from the systemic circulation. For type 2 diabetes patients, stabilizing blood glucose levels is a critical factor in the treatment (36). Encapsulating Exe into dimpled PLGA-MPs achieved sustained drug release for 3 weeks *in vivo* and enhanced bioavailability after a single injection, which could significantly reduce the frequency of administration and potential risks induced by fluctuation in glucose levels as well as improve the patient compliance. Compared to the daily (Byetta®) and weekly (Bydureon™) formulations of Exe in the market, Exe loaded dimpled PLGA-MPs could have great potential in clinical application for the long-term treatment of type 2 diabetes.

## CONCLUSION

Exe-PLGA-MPs were successfully prepared by UPPS with dimpled shapes, uniform particle sizes, and a high EE%. Compared to spherical MPs, dimpled MPs achieved sustained drug release over 2 months *in vitro* with almost constant drug release rate and reduced initial burst due to their large surface area. The bioactivity of Exe was not affected by the preparation process of MPs with the secondary structure of encapsulated Exe well maintained. Moreover, the pharmacokinetic results suggested that Exe was slowly released from dimpled PLGA-MPs for 3 weeks *in vivo* after a single injection, which was bioequivalent to administration of Exe solution. Therefore, PLGA-MPs prepared by UPPS could have great potential for sustained delivery of Exe in the treatment of type 2 diabetes.

## FUNDING INFORMATION

This work was funded by the China Postdoctoral Science Foundation (Grant No. 2016M602442), the Natural Science Fund Project of Guangdong Province (Grant No. 2018A030310555, 2016A030312013).

## COMPLIANCE WITH ETHICAL STANDARDS

This study was approved by the Ethical Committee on Animal Experimentation at Sun Yat-sen University.

**Conflict of Interest** The authors declare that there is no conflict of interest.

**Abbreviations** DCM, dichloromethane; DMC, dimethyl carbonate; DL%, drug loading; EE%, encapsulation efficiency; Exe-PLGA-MPs, exenatide loaded PLGA-MPs; GLP-1, glucagon-like peptide-1; *IVIVC*; *in vitro-in vivo* correlations; MPs, microparticles; MRT, mean residence time; PLGA, D, L-lactic-co-glycolic acid; RB%, relative bioavailability; SD, Sprague-Dawley; SDS-PAGE, sodium dodecyl sulfate-polyacrylamide gel electrophoresis; SR-μCT, synchrotron radiation X-ray computed microtomography; S/O/W, solid in oil in water; UPPS, ultra-fine particle processing system; W/O, water in oil; W/O/O, water in oil in oil; W/O/W, water in oil in water.



## REFERENCES

1. Hirota K, Doty AC, Ackermann R, Zhou J, Olsen KF, Feng MR, et al. Characterizing release mechanisms of leuprolide acetate-loaded PLGA microspheres for IVIVC development I: *In vitro* evaluation. J Control Release. 2016;244:302–13. https://doi.org/10.1016/j.jconrel.2016.08.023.
2. Qi F, Wu J, Yang TY, Ma GH, Su ZG. Mechanistic studies for monodisperse exenatide-loaded PLGA microspheres prepared by different methods based on SPG membrane emulsification. Acta Biomater. 2014;10(10):4247–56. https://doi.org/10.1016/j.actbio.2014.06.018.
3. Martin-Sabroso C, Fraguas-Sanchez AI, Aparicio-Blanco J, Cano-Abad MF, Torres-Suarez AI. Critical attributes of formulation and of elaboration process of PLGA-protein microparticles. Int J Pharm. 2015;480(1–2):27–36. https://doi.org/10.1016/j.ijpharm.2015.01.008.
4. Versypt ANF, Pack DW, Braatz RD. Mathematical modeling of drug delivery from autocatalytically degradable PLGA microspheres - a review. J Control Release. 2013;165(1):29–37. https://doi.org/10.1016/j.jconrel.2012.10.015.
5. Peters T, Kim SW, Castro V, Stingl K, Strasser T, Bolz S, et al. Evaluation of polyesteramide (PEA) and polyester (PLGA)

microspheres as intravitreal drug delivery systems in albino rats. Biomaterials. 2017;124:157–68. https://doi.org/10.1016/j.biomaterials.2017.02.006.
6. Ahn JH, Park EJ, Lee HS, Lee KC, Na DH. Reversible blocking of amino groups of octreotide for the inhibition of formation of acylated peptide impurities in poly (lactide-co-glycolide) delivery systems. AAPS PharmSciTech. 2011;12(4):1220–6. https://doi.org/10.1208/s12249-011-9694-y.
7. Wang H, Zhang GX, Ma XQ, Liu YH, Feng J, Park K, et al. Enhanced encapsulation and bioavailability of breviscapine in PLGA microparticles by nanocrystal and water-soluble polymer template techniques. Eur J Pharm Biopharm. 2017;115:177–85. https://doi.org/10.1016/j.ejpb.2017.02.021.
8. Chen L, Mei L, Feng D, Huang D, Tong X, Pan X, et al. Anhydrous reverse micelle lecithin nanoparticles/PLGA composite microspheres for long-term protein delivery with reduced initial burst. Colloid Surf B. 2017;163:146–54. https://doi.org/10.1016/j.colsurfb.2017.12.040.
9. Ye ML, Kim S, Park K. Issues in long-term protein delivery using biodegradable microparticles. J Control Release. 2010;146(2):241–60. https://doi.org/10.1016/j.jconrel.2010.05.011.
10. Ramazani F, Chen WL, van Nostrum CF, Storm G, Kiessling F, Lammers T, et al. Strategies for encapsulation of small hydrophilic and amphiphilic drugs in PLGA microspheres: state-of-the-art and challenges. Int J Pharm. 2016;499(1–2):358–67. https://doi.org/10.1016/j.ijpharm.2016.01.020.
11. Houchin ML, Topp EM. Chemical degradation of peptides and proteins in PLGA: a review of reactions and mechanisms. J Pharm Sci. 2008;97(7):2395–404. https://doi.org/10.1002/jps.21176.
12. Wen XG, Peng XS, Fu H, Dong YX, Han K, Su JF, et al. Preparation and *in vitro* evaluation of silk fibroin microspheres produced by a novel ultra-fine particle processing system. Int J Pharm. 2011;416(1):195–201. https://doi.org/10.1016/j.ijpharm.2011.06.041.
13. Zhu CE, Huang Y, Zhang XY, Mei LL, Pan X, Li G, et al. Comparative studies on exenatide-loaded poly (D,L-lactic-co-glycolic acid) microparticles prepared by a novel ultra-fine particle processing system and spray drying. Colloid Surf B. 2015;132:103–10. https://doi.org/10.1016/j.colsurfb.2015.05.001.
14. Huang ZW, Chen XN, Fu H, Wen XG, Ma C, Zhang JW, et al. Formation mechanism and *in vitro* evaluation of risperidone-containing PLGA microspheres fabricated by ultrafine particle processing system. J Pharm Sci. 2017;106(11):3363–71. https://doi.org/10.1016/j.xphs.2017.07.010.
15. Mentz RJ, Bethel MA, Gustavson S, Thompson VP, Pagidipati NJ, Buse JB, et al. Baseline characteristics of patients enrolled in the exenatide study of cardiovascular event lowering (EXSCEL). Am Heart J. 2017;187:1–9. https://doi.org/10.1016/j.ahj.2017.02.005.
16. Chatterjee S, Khunti K, Davies MJ. Type 2 diabetes. Lancet. 2017;389(10085):2239–51. https://doi.org/10.1016/S0140-6736(17)30058-2.
17. Zhang Y, Zhong Y, Hu M, Xiang NX, Fu Y, Gong T, et al. *In vitro* and *in vivo* sustained release of exenatide from vesicular phospholipid gels for type II diabetes. Drug Dev Ind Pharm. 2016;42(7):1042–9. https://doi.org/10.3109/03639045.2015.1107090.
18. Ni R, Muenster U, Zhao J, Zhang L, Becker-Pelster EM, Rosenbruch M, et al. Exploring polyvinylpyrrolidone in the engineering of large porous PLGA microparticles via single emulsion method with tunable sustained release in the lung: *In vitro* and *in vivo* characterization. J Control Release. 2017;249:11–22. https://doi.org/10.1016/j.jconrel.2017.01.023.
19. Pelton JT, McLean LR. Spectroscopic methods for analysis of protein secondary structure. Anal Biochem. 2000;277(2):167–76. https://doi.org/10.1006/abio.1999.4320.
20. Wang PX, Wang Q, Ren TY, Gong HY, Gou JX, Zhang Y, et al. Effects of Pluronic F127-PEG multi-gel-core on the release profile and pharmacodynamics of exenatide loaded in PLGA microspheres. Colloid Surf B. 2016;147:360–7. https://doi.org/10.1016/j.colsurfb.2016.08.032.
21. Guo Z, Yin XZ, Liu CB, Wu L, Zhu WF, Shao Q, et al. Microstructural investigation using synchrotron radiation X-ray microtomography reveals taste-masking mechanism of acetaminophen microspheres. Int J Pharm. 2016;499(1–2):47–57. https://doi.org/10.1016/j.ijpharm.2015.12.045.
22. Qi F, Wu J, Hao DX, Yang TY, Ren Y, Ma GH, et al. Comparative studies on the influences of primary emulsion preparation on properties of uniform-sized exenatide-loaded PLGA microspheres. Pharm Res. 2014;31(6):1566–74. https://doi.org/10.1007/s11095-013-1262-6.
23. Lin YQ, Khetarpal R, Zhang YL, Song HC, Li SS. Combination of ELISA and dried blood spot technique for the quantification of large molecules using exenatide as a model. J Pharmacol Toxicol Methods. 2011;64(2):124–8. https://doi.org/10.1016/j.vascn.2011.04.004.
24. Kothare PA, Linnebjerg H, Isaka Y, Uenaka K, Yamamura A, Yeo KP, et al. Pharmacokinetics, pharmacodynamics, tolerability, and safety of exenatide in Japanese patients with type 2 diabetes mellitus. J Clin Pharmacol. 2008;48(12):1389–99. https://doi.org/10.1177/0091270008323750.
25. Furtado S, Abramson D, Simhkay L, Wobbekind D, Mathlowitz E. Subcutaneous delivery of insulin loaded poly (fumaric-co-sebacic anhydride) microspheres to type 1 diabetic rats. Eur J Pharm Biopharm. 2006;63(2):229–36. https://doi.org/10.1016/j.ejpb.2005.12.012.
26. Xuan JM, Lin YL, Huang JB, Yuan F, Li XQ, Lu Y, et al. Exenatide-loaded PLGA microspheres with improved glycemic control: *In vitro* bioactivity and *in vivo* pharmacokinetic profiles after subcutaneous administration to SD rats. Peptides. 2013;46:172–9. https://doi.org/10.1016/j.peptides.2013.06.005.
27. Kim JY, Lee H, Oh KS, Kweon S, Jeon OC, Byun Y, et al. Multilayer nanoparticles for sustained delivery of exenatide to treat type 2 diabetes mellitus. Biomaterials. 2013;34(33):8444–9. https://doi.org/10.1016/j.biomaterials.2013.07.040.
28. Oh KS, Kim JY, Yoon BD, Lee M, Kim H, Kim M, et al. Sol-gel transition of nanoparticles/polymer mixtures for sustained delivery of exenatide to treat type 2 diabetes mellitus. Eur J Pharm Biopharm. 2014;88(3):664–9. https://doi.org/10.1016/j.ejpb.2014.08.004.
29. Fang LW, Yin XZ, Wu L, He YP, He YZ, Qin W, et al. Classification of microcrystalline celluloses via structures of individual particles measured by synchrotron radiation X-ray micro-computed tomography. Int J Pharm. 2017;531(2):658–67. https://doi.org/10.1016/j.ijpharm.2017.05.019.
30. Ju XJ, Wang XX, Liu Z, Xie R, Wang W, Chu LY. Red-blood-cell-shaped chitosan microparticles prepared by electrospraying. Particuology. 2017;30:151–7. https://doi.org/10.1016/j.partic.2016.05.011.
31. Panyam J, Dali MA, Sahoo SK, Ma WX, Chakravarthi SS, Amidon GL, et al. Polymer degradation and *in vitro* release of a model protein from poly(D,L-lactide-co-glycolide) nano- and microparticles. J Control Release. 2003;92(1–2):173–87. https://doi.org/10.1016/S0168-3659(03)00328-6.
32. Wang H, Zhang GX, Sui H, Liu YH, Park K, Wang WP. Comparative studies on the properties of glycyrrhetinic acid-loaded PLGA microparticles prepared by emulsion and template methods. Int J Pharm. 2015;496(2):723–31. https://doi.org/10.1016/j.ijpharm.2015.11.018.
33. Wang PX, Zhuo XZ, Chu W, Tang X. Exenatide-loaded microsphere/ thermosensitive hydrogel long-acting delivery system with high drug bioactivity. Int J Pharm. 2017;528(1–2):62–75. https://doi.org/10.1016/j.ijpharm.2017.05.069.
34. Doshi N, Zahr AS, Bhaskar S, Lahann J, Mitragotri S. Red blood cell-mimicking synthetic biomaterial particles. Proc Natl Acad Sci U S A. 2009;106(51):21495–9. https://doi.org/10.1073/pnas.0907127106.
35. Doty AC, Zhang Y, Weinstein DG, Wang Y, Choi S, Qu W, et al. Mechanistic analysis of triamcinolone acetonide release from PLGA microspheres as a function of varying *in vitro* release conditions. Eur J Pharm Biopharm. 2017;113:24–33. https://doi.org/10.1016/j.ejpb.2016.11.008.
36. Lim SM, Eom HN, Jiang HH, Sohn M, Lee KC. Evaluation of PEGylated exendin-4 released from poly (lactic-co-glycolic acid) microspheres for antidiabetic therapy. J Pharm Sci. 2015;104(1):72–80. https://doi.org/10.1002/jps.24238.